Article

A Comparison of Numerical Approaches for the Design of Mooring Systems for Wave Energy Converters

Imanol Touzon [1,2,*], **Vincenzo Nava** [3,4], **Borja de Miguel** [1] **and Victor Petuya** [2]

[1] IDOM Engineering, Consulting and Architecture S.A.U., Av. Zarandoa 23, 48015 Bilbao, Spain; bdemiguel@idom.com
[2] Department of Mechanical Engineering, University of the Basque Country–UPV/EHU, 48013 Bilbao, Spain; victor.petuya@ehu.es
[3] Tecnalia, Basque Research and Technology Alliance (BRTA), Edificio 700, 48160 Derio, Bizkaia, Spain; vincenzo.nava@tecnalia.com
[4] Basque Centre for Applied Mathematics, BCAM, 48009 Bilbao, Spain
* Correspondence: imanol.touzon@idom.com

check for
updates

Abstract: This paper analyses the numerical outcome of applying three different well-known mooring design approaches to a floating wave energy converter, moored by means of four catenary lines. The approaches include: a linearized frequency domain based on a quasistatic model of the mooring lines, a time domain approach coupled with an analytic catenary model of the mooring system, and a fully coupled non-linear time domain approach, considering lines' drag and inertia forces. Simulations have been carried out based on a set of realistic combinations of lines pretension and linear mass, subject to extreme environmental conditions. Obtained results provide realistic cost and performance indicators, presenting a comparison in terms of total mooring mass and required footprint, as well as the design line tension and structure offset. It has been found that lines' viscous forces influence significantly the performance of the structure with high pretensions, i.e., >1.2, while there is acceptable agreement between the modelling approaches with lower pretensions. Line tensions are significantly influenced by drag and inertia forces because of the occurrence of snap loads due to the heaving of the floater. However, the frequency domain approach provides an insight towards the optimal design of the mooring system for preliminary designs.

Keywords: catenary mooring system; linear hydrodynamics; dynamic mooring lines; wave energy conversion

1. Introduction

The early stage design of mooring systems for offshore floating wave energy technologies is affected by high uncertainty of the estimated required investment. Such uncertainty arises when simplistic models are used to account for the station-keeping system, especially when floating moored structures are more dynamic and smaller than those of the traditional offshore industry.

Mooring impact on cost of energy is estimated to be of around 10% of the capital expenditure (CAPEX) [1]. It is therefore decisive to make appropriate estimations of the mooring performance and cost from an early stage of development of these technologies so that realistic levelized cost of energy forecasts can be obtained.

The suggested methods in the offshore standards [2,3] consider different physical phenomena such as non-linear static catenary mooring systems or fully non-linear lines, including lines' inertia and drag forces. The simplest model consists in considering the mooring system influence on the structure

through the tangent stiffness at the mean position, just on translational modes of motion (surge and sway) [2]. The resulting stiffness is added to the hydrostatic stiffness matrix and floaters' motions are computed in the frequency domain (FD). This approach is denoted here as quasistatic-frequency domain method (QSFD). It is recommended [3] to simulate the floating structure low frequency motions in the time domain coupled with the analytical catenary equations, which provides a force in all degrees of freedom every time step of the simulation. This method introduces the non-linear geometric stiffness in floaters' motions, unlike the previous model in which it was linearized. This approach is denoted here as the quasistatic-time domain method (QSTD). The most sophisticated model, and in turn time consuming, consists in accounting for the non-linear geometric stiffness as well as lines' drag and inertia forces in the time domain, fully coupled with the structure. This approach is denoted here as the dynamic time domain method (DynTD).

Mooring system influence on the structure can be easily estimated via the QSFD method as well as its design tension subject to specific environmental states. However, not accounting for the non-linear geometric stiffness and lines' dynamics may introduce a large uncertainty in structure and mooring performance estimations, which must be accounted for through appropriate safety factors. Some authors have already compared the differences between simulation in the time domain with the QSTD compared with the DynTD. A maximum tension ratio between 2 and 3 of the equivalent DynTD model with respect to the equivalent QSTD for regular waves depending on the oscillation period of the fairlead was documented [4]. An underprediction of the equivalent QSTD model of maximum line tensions of 60% to 70% under regular motions has been documented [5] with respect to experimental tests. In addition to the accuracy of different approaches, it has been found [6] that inaccuracies in structure motions are directly translated into differences on mooring line tensions. However, the QSTD approach has been successfully applied to estimate the umbilical cable influence on underwater vehicles [7,8], accounting for current forces on the umbilical. Other studies [9] have analysed the influence of considering hydrodynamic loads, closely related with the drag forces, on lines with the DynTD approach, resulting in an increase on line tensions.

Wave energy conversion has extensively been investigated so far and many concepts have been studied [10]. Among them, the Oscillating Water Column (OWC) device type is one of the most promising technologies. It has been extensively analysed [11–13] and several demonstration deployments have been carried out, both as fixed [14,15] and as floating [16] devices.

The present work aims to identify the main sources of discrepancy among the three above-mentioned approaches for a set of realistic combinations of line mass and pretensions. A comparison based on numerical simulations is introduced to give an insight into the accuracy of the estimation of structure offset, maximum tension, total mooring mass, and the required footprint, applied to a spar type floating wave energy converter (FWEC). These parameters provide information to be considered in a global perspective together with other CAPEX indicators and production revenues, so that the design of the whole device can be kept optimised from early stages.

2. Numerical Models

Three numerical models are here introduced to account for different non-linear effects so that a comparison can be carried out in terms of performance (structure motions and line tensions) and cost indicators (required footprint and total mooring mass). Hydrodynamics are based on linear potential theory with a non-linear viscous drag force added in all degrees of freedom. Many codes based on linear potential flow have been developed and compared [17,18] in order to assess the power production of FWECs. Nevertheless, the influence of viscous forces are increasingly significant as the incoming wave energy is increased, as well as the non-linear Froude-Krylov forces [19]. Here, a viscous damping term has been considered for simplicity since the scope of the paper is to enable a comparison between numerical models. Drift force is computed using the Newman approximation, whilst the current force has been considered constant. Mooring performance model is included in the numerical model in a different manner in each of the three models, subsequently introduced.

2.1. Quasistatic Mooring Frequency Domain

This method is introduced [2] for traditional offshore structures, provided it is demonstrated that effects from anchor line dynamics are negligible. It consists in linearizing the horizontal restoring force of the mooring system at the estimated mean position based on steady mean forces, i.e., mean current force and mean drift force. A horizontal stiffness is introduced in the surge/sway motion and the equation of motion (1) is solved in the frequency domain to obtain the response amplitude vector $\{\delta_a(\omega)\}$ subject to the wave force amplitude vector $\{\hat{F}_w(\omega)\}$:

$$\left[-\omega^2[M + A(\omega)] + i\omega[B(\omega) + B_d] + [H + K_m]\right]\cdot\{\hat{\delta}_a(\omega)\} = \{\hat{F}_w(\omega)\} \tag{1}$$

where:

$[M]$: Mass matrix of the floating structure
$[A(\omega)]$: Added mass matrix
$[B(\omega)]$: Radiation damping matrix
$[B_d]$: Linearized drag force
$[H]$: Hydrostatic matrix
$[K_m]$: Linearized mooring stiffness

It is solved separately for wave frequency and low frequency motions. The vector $\{\hat{F}_w(\omega)\}$ is therefore replaced by the Froude-Krylov and diffraction amplitude excitation force of the sea state $S_\tau(\omega)$, for wave frequency (WF) motions, and by the corresponding force amplitude presented by Pinkster [20], for slowly varying low frequency wave drift forces, specified in Equation (2).

$$S_{SV}(\mu) = 8\cdot\int_0^\infty S_\tau(\omega + \mu)\cdot S_\tau(\omega)\cdot|T(\omega + \mu, \omega)|^2\cdot d\omega \tag{2}$$

where:

$S_{SV}(\mu)$: Slowly-varying wave drift force spectrum
$T(\omega, \omega)$: Drift force quadratic transfer function

The characteristic tension in which this paper is based is computed from a combination of horizontal motions of both frequency ranges, as shown in Equation (3):

$$\delta_{char} = max\left(\delta_{sig}{}^{LF} + \delta_{max}{}^{WF}; \delta_{max}{}^{LF} + \delta_{sig}{}^{WF}\right) \tag{3}$$

where:

$$\delta_{sig} = 2\cdot\sigma_x \quad and \quad \delta_{max} = \sigma_x\cdot\sqrt{2\cdot ln(N)} \tag{4}$$

$$T_{d\_QSFD} = T(\delta_{mean} + \delta_{char}) \tag{5}$$

And σ_x is the standard deviation in surge, N the number of oscillations during the duration of the environmental state, and T_{d_QSFD} the design tension with this approach.

The corresponding line tension is provided by the catenary equations for the mooring system at the characteristic offset (δ_{char}) added to the mean offset.

In this paper, the static line tension, suspended length, and offset of the structure have been non-dimensionalised as carried out in [21] in order to characterize the mooring configuration, and apply them into the QSFD approach. The non-dimensional pretensions represent, for a given axial stiffness, the shape of mooring lines with the structure at the origin; see Figure 1. It assumed that all lines are equal for simplicity. It enables an easy coupling of the catenary mooring system with the surge motion of any structure, line mass, line stiffness, and water depth. In order to do that, several non-dimensional pretensions (see Equation (6)) for different axial stiffness values have been computed

with the analytic catenary equations; where T_i is the line's pretension, l_s the suspended length, and w the linear weight. An example of different line shapes for varying non-dimensional pretension (2.4613–1.0059) is provided in Figure 1.

$$a_i = \frac{T_i\ [N]}{l_s[m] \cdot w\left[\frac{N}{m}\right]} \tag{6}$$
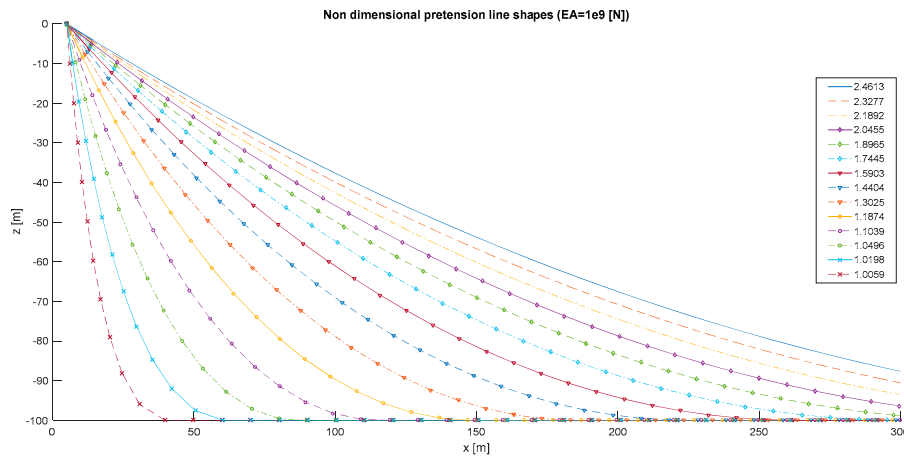
Figure 1. Non-dimensional pretension line shapes for axial stiffness EA = 1e9 [N].

Other linearized models have been applied by several authors ([22–24]), including line dynamics in linearized models with certain accuracy under specific conditions. However, they are more sophisticated and are not yet collected in recognized standards, being therefore out of the scope of this work.

2.2. Quasistatic Mooring Time Domain

This modelling method is proposed in [3] and consists of solving the Cummins [25] equation of motion (7) coupled with the catenary mooring force $\{F_m(t)\}$ in all degrees of freedom. The convolution term for the radiation damping has been solved through direct numerical integration. This model is advantageous since it considers the non-linear geometric stiffness of the catenary lines making up the mooring system as well as the influence of all degrees of freedom in the mooring line tension. However, it requires catenary equations to be solved at every time step with its implicit iterative loop.

$$[M + A_\infty] \cdot \{\ddot{\delta}(t)\} + \left\{ \int_{-\infty}^{t} B(t-\tau) \cdot \dot{\delta}(\tau) \cdot d\tau \right\} + [H] \cdot \{\delta(t)\} = \{F_w(t)\} + \{F_m(t)\} + \{F_d(t)\} \tag{7}$$

The term $\{F_d(t)\}$ represents the viscous drag force on the structure, modelled for each degree of freedom as in Equation (8):

$$F_d(t) = -C_i \cdot \dot{\delta}_i(t) \cdot \left| \dot{\delta}_i(t) \right| \tag{8}$$

where 'i' denotes the degree of freedom and C_i the corresponding drag force factor, as specified in Table 3.

In this work, the mooring system has been represented by the elastic catenary equations with zero touch-down angle [21]. To represent all statistical properties of the low frequency (LF) motions, at least five three-hour-long simulations [3] have been performed. The maximum line tension of each

simulation T_k is processed as represented with Equations (9) and (10), where 'n' refers to the number of simulations and T_{d_QSTD} is the design tension with this approach.

$$T_\mu = \frac{1}{n}\sum_{k=1}^{n} T_k \quad ; \quad T_\sigma = \sqrt{\frac{1}{n}\sum_{k=1}^{n}\left(T_k - T_\mu\right)^2} \tag{9}$$

$$T_{d\_QSTD} = T_\mu + 2 \cdot T_\sigma \tag{10}$$

where:

T_μ: Mean line tension
T_σ: Standard deviation of line tension maxima of the set of simulations

2.3. Dynamic Mooring Time Domain

The third approach consists of modelling the mooring lines through the non-linear finite element method coupled with the structure motions, modelled here through the linear potential theory. Water waves' forces on lines are accounted for through the Morison equation and seabed interaction with discrete springs and dampers, representing soil properties. Such a method, initially introduced by [26], has been implemented and currently available in the commercial software Orcaflex [27].

The maximum line tension is computed assuming a Gumbel distribution for the maxima of the simulations as specified in Equation (11). In order to represent the low frequency variations, it is recommended in [2] to carry out at least ten 3-h time domain simulations.

$$T_{d\_DynTD} = T_\mu - 0.577216 \cdot T_\sigma \cdot \frac{\sqrt{6}}{\pi} \tag{11}$$

where T_μ and T_σ are the mean and the standard deviation of the maximum line tensions of the 10 simulations, respectively, and T_{d_DynTD} the design line tension with this approach.

Even though this model is the most extensively used due to its accuracy and availability of commercial codes such as [27], it may be too time-consuming for sensitivity analyses of cost indicators, which is dealt with along this paper.

2.4. Reference Simulation Cases

To design a mooring system for a FWEC, ultimate limit state (ULS) loads are to be accounted for with the device in the survival mode. There are multiple simulation combinations that may appear in real environments; however, in an early stage of development a worst-case scenario can be initially selected in order to get estimations of both performance and cost indicators.

A single load case has been simulated with multiple combinations of lines' non-dimensional pretension and linear mass. The outcomes provide information about performance (maximum offset and design line tension) and cost (mooring mass and required footprint) indicators.

A sensitivity analysis was carried out with both QSTD and DynTD models in order to define the simulation settings. The DynTD model, made in Orcaflex [27], has been analyzed with lines made up of 10 to 100 elements and the relative errors have been in all cases below 5%. The number of elements considered for the presented results have been 80 and a time step of 0.1 s.

The QSTD model results are subject to the error allowed in the iterative process involved in the catenary equations. A sensitivity analysis has been carried out with the model presented in the previous section in order to check the accuracy of the mooring force with different relative errors allowed in the iterative loop.

It is shown in Figure 2 that both line tension and structure horizontal position relative errors are found below 5% for a maximum allowed error in the catenary equations of 0.2%, assumed to be

sufficiently accurate. This model has been proved to provide accurate results when using a time step of 0.1 s with a Newmark-beta integration scheme [28].

(a)

(b)
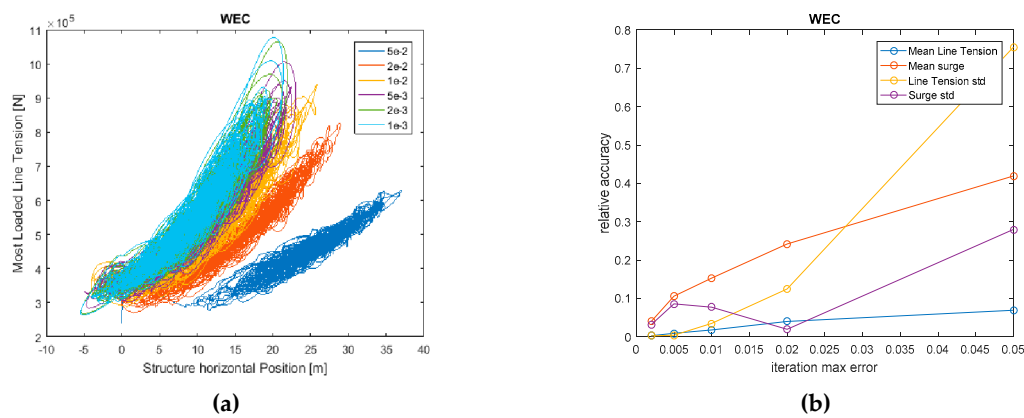
Figure 2. Sensitivity analysis of the QSTD model to the iterative process of the catenary equations. Surge of the structure and the corresponding mooring horizontal force (**a**) and relative errors of the standard deviation with different relative errors allowed in the catenary equations of both line tension and surge motion (**b**).

2.5. Environmental Conditions

The simulation reference selected case corresponds to the combination of the recommended environmental conditions for permanent traditional offshore structures [2], at the test site bimep [29], and specified in Table 1.

Table 1. Environmental conditions for the reference simulation case.

Parameter	Return Period	Value
Significant Wave Height	100 yrs	10 m
Peak Period (Tp)		18 s
Current Velocity (Vc)	50 yrs	1.3 m/s

The environmental data has been taken from [29], where an analysis of extreme climate conditions is presented for the site. The current velocity has been assumed constant over the depth of the floating WEC and the spectral shape used in the analysis has been JONSWAP with a peak shape parameter equal to 3.3. The corresponding load case assumes that waves, wind, and current are all aligned with one line of the mooring system. The wind force has not been considered for simplicity; therefore, the corresponding extreme value has been omitted in Table 1.

2.6. Mooring Properties

The mooring system represented in the numerical model is a four-line catenary mooring system with the lines radially regularly distributed, as represented in Figure 3. The fairleads of the mooring lines have been assumed to be located at the same height of the center of gravity of the FWEC to keep the stability in pitch of the buoy and avoid additional couplings between surge, heave, and pitch.
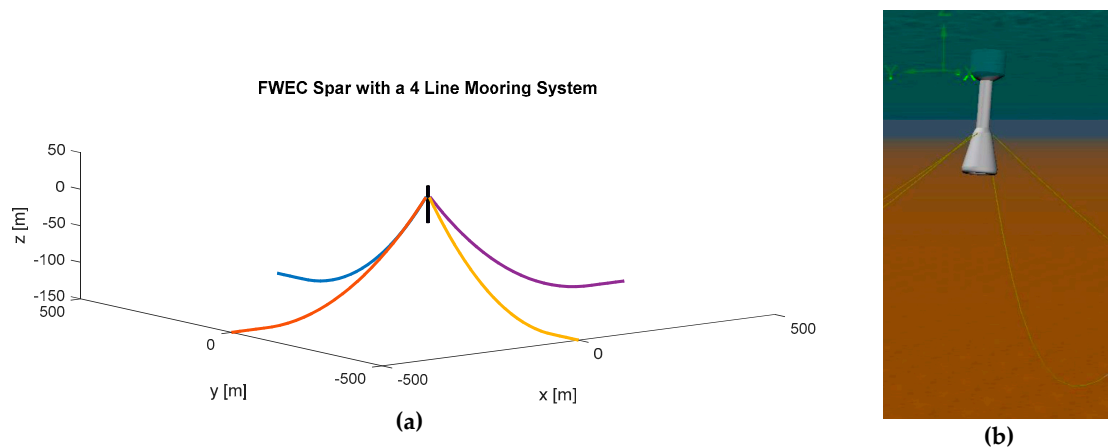
Figure 3. Four lines mooring system configuration modeled for both structures in 150 m water depth. Visualization of the QSTD model developed on Matlab [30] (**a**) and the DynTD model on Orcaflex [27] (**b**).

In order to find to what extent non-linearities of the mooring system influence the structure motions and line tensions, a range of realistic non-dimensional pretensions, as defined in Equation (6), and linear mass has been defined as specified in Table 2, which results in 25 mooring models.

Table 2. Mooring properties selected to be combined for simulation cases, resulting in 25 cases arisen from combining each linear mass with each non-dimensional pretension.

| Mooring Linear Mass [kg/m]	Non-Dimensional Pretension [-]	Length/Mass Number
65	1.43	1
85	1.26	2
105	1.16	3
125	1.10	4
145	1.06	5

The vertical coordinate of the fairlead of the mooring lines with respect to the seabed has been assumed to be 150 m, assuming the fairleads at the center of gravity. Therefore, the resulting water depth is 181.97 m. It should be noted that the four mooring lines have been assumed to be of equal length for simplicity; however, detailed designs lines might result in different lengths if the probability of waves' direction is accounted for. Therefore, the cost indicators to be introduced here must be seen as an upper bound provided for preliminary designs.

2.7. Numerical Model of the Floating Wave Energy Converter

The FWEC geometry is based on the optimization presented in [11], model 'K'. It has also been modelled through linear potential theory and its mesh representation and main dimensions are shown in Figure 4.

This geometry is designed to work as an OWC in which the power is extracted from the relative heaving motion of the represented structure in Figure 4 with respect to the internal water column. The compressed and expanded air is made to pass through a self-rectifying air turbine allocated on the top deck of the floating structure. Its hydrodynamic properties for power production assessment can be modelled, among other methods, through two oscillating bodies. The coupled model consists of the one represented in Figure 4 interacting with a massless surface representing the free surface water of the internal water column. In this paper, ULS is assessed, and it is assumed that the survival mode of operation can be approximated by the structure open at its top part. Therefore, the hydrodynamic model has been built up based on a single body, representing the structure.
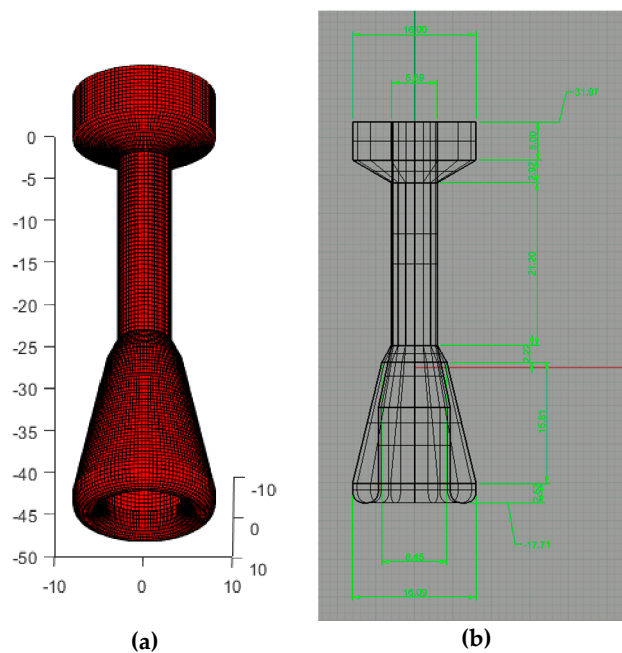
Figure 4. Mesh representation of the boundary element method (BEM) model for the FWEC spar platform submerged part (**a**) and its main dimensions [m] with the reference at its CoG (**b**). Reproduced from [11] (Renewable Energy 44 (2012) 328–339), corresponding to model 'K'.

The current steady force has been applied through a drag coefficient of 0.65 with an associated surface of 290 [m^2]. Its total mass is 2.434×10^6 [kg].

The quadratic damping force to account for the viscous damping has been considered adding the factors in Table 3, computed assuming a common drag coefficient for cylinders of Cd = 0.8 [31].

Table 3. Viscous force factors used for the FWEC.

Degree of Freedom	Viscous Force Factor
Surge [N·s/m]	1.188×10^5
Sway [N·s/m]	1.188×10^5
Heave [N·s/m]	4.469×10^4
Roll [N·m·s]	3.532×10^9
Pitch [N·m·s]	3.532×10^9
Yaw [N·m·s]	0

The non-linear drift force has been accounted for through the Newman approximation and based on the mean drift coefficients computed by the linear potential code.

3. Results

Results of the performance and cost indicators are introduced in this section. In order to compare the influence of the non-linear effects, the QSFD results have been considered as a baseline whilst the results of both DynTD and QSTD models are compared with the baseline.

3.1. Quasistatic Frequency Domain Model Results

In this approach, the horizontal stiffness computed at the mean position is added to the hydrostatic matrix to obtain the solution amplitudes. This method allows computing natural frequencies of the degrees of freedom of the structure. Since the mooring settings are variable, natural frequency in surge

may vary between 0.03 rad/s and 0.07 rad/s. Natural frequencies of the structure in heave and pitch without mooring system have been found to be 0.67 rad/s and 0.38 rad/s, respectively.

Main performance factors to be considered when designing a mooring system are the maximum line tension and the maximum structure horizontal displacement. These parameters are relevant for the mooring system and umbilical cable structural integrity.

Each line in Figure 5 represents a linear mass of the lines composing the mooring system and the variation of each performance and cost indicator along each linear mass is due to the variation in the non-dimensional pretension, within the values specified in Table 2. A non-dimensional pretension (a_i) increase produces larger anchor radius (R_anchor) and lower design offset (X_d) in all cases.

A pretension increase influences the offset of the structure independently of the line mass; however, it also increases significantly the design tension, which may lead to unsafe designs as shown in Figure 5 (left). The design offset of the structure is very sensitive to the linear mass at mid-low pretensions; however, with large pretensions, i.e., $a_i > 1.2$, the variation of the offset due to the linear mass (65 kg/m–145 kg/m) becomes less significant.

Large pretensions imply in general larger footprints and total mooring mass, that are eventually translated into larger total costs of the mooring system. Similarly to what is observed for the offset, the anchor radius is very sensitive to the linear mass at mid-low pretensions; however, with high pretensions, the impact on the anchor radius is significantly lower, which is represented in Figure 5 (right).

It should be pointed out that these baseline results indicate a requirement in the mooring total mass of 5–15% the mass of the structure, as long as lines are completely made up of a single chain type.
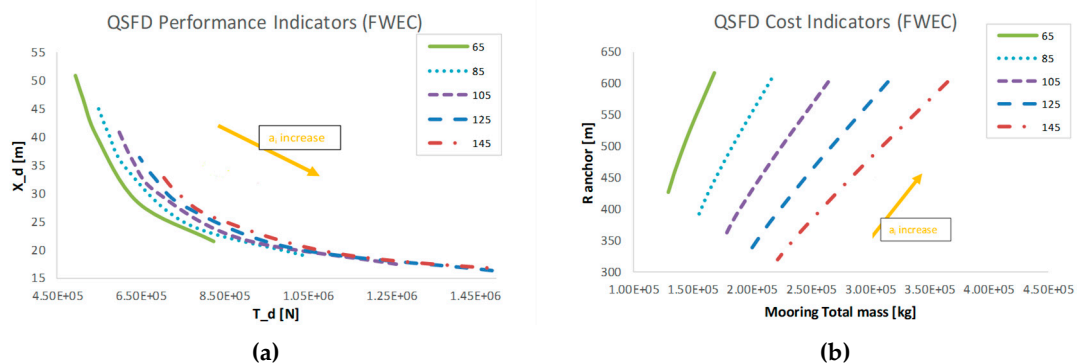
Figure 5. Baseline results of the QSFD model. Performance indicators of line design tension and design offset (**a**) and cost indicators of mooring total mass and anchor radius (**b**).

3.2. Performance Results of Non-Linear QSTD and DynTD Models

To quantify the uncertainty of the QSFD baseline indicators, results of both time domain models are introduced as factors with respect to the indicators introduced in Figure 5. It enables quantifying the influence of non-linear effects such as the geometric stiffness or lines' drag and inertia as well as coupling all degrees of freedom with the mooring system. In addition to the geometric stiffness and the mooring influence on all degrees of freedom, accounted for in the QSTD model, lines' drag and inertia forces are also considered in the DynTD model.

Floater Dynamics

The most significantly excited degrees of freedom in the introduced numerical models are surge, heave, and pitch motions since all environmental forces have been aligned and propagated along the positive 'x' axis. These directly influence line tensions and the structural integrity of the umbilical cable that any WEC must have installed in order to transport electrical energy. These components are specially influenced by the surge motion of the structure, which corresponds to the horizontal offset in the case study here defined.

　　　The FWEC shows in Figure 6a balanced influence between the mean and dynamic surge on the design offset factors. Mean offset contribution is significantly increased as the non-dimensional pretension is decreased with slightly higher influence in the QSTD model. The total offset factor is dominated by structure dynamics with large non-dimensional pretensions and by the mean offset with low non-dimensional pretensions.
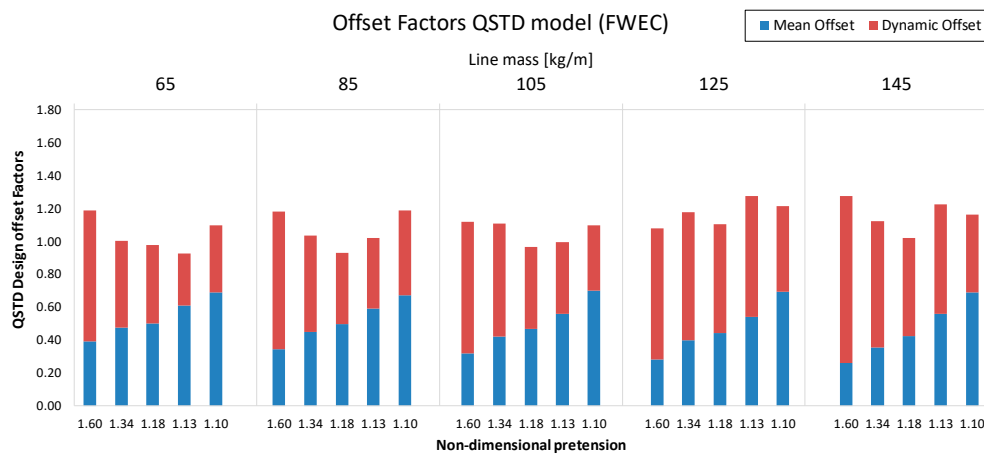
(a)
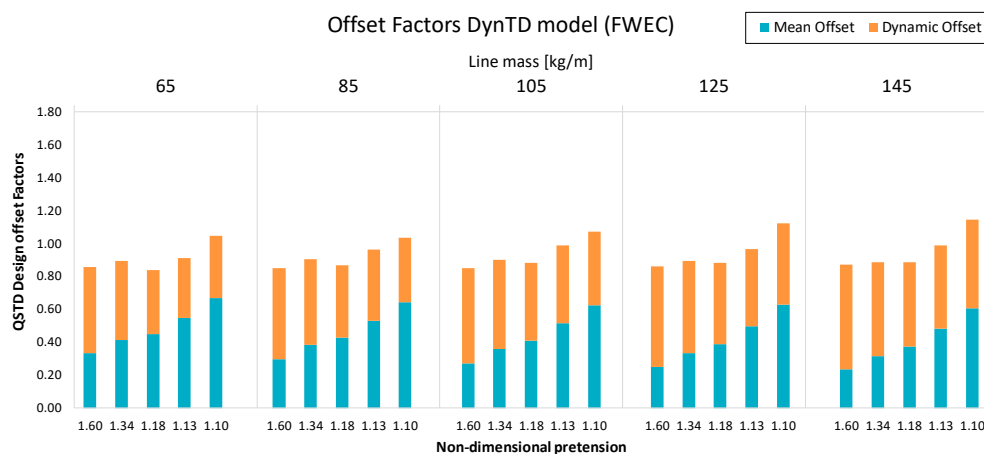
(b)

Figure 6. Surge factors with respect to QSFD model of the QSTD (**a**) and DynTD (**b**) approaches. Accumulated bars with the weights of the mean and dynamic offsets.

　　　It is to be noted that most mooring models show factors <1 for the design offset with the DynTD model, whilst the QSTD model shows factors >1. It indicates, assuming that the most reliable model is the DynTD, that the QSFD model is more conservative in the estimation of the characteristic offsets of the structure rather than the QSTD for this kind of FWECs.

　　　Design offset values shown in Figure 6 have been estimated through the same procedure as carried out for lines tensions in each model, described in Equations (3) to (11).

　　　Factors of the QSTD approach in terms of heave and pitch std have been omitted as they show almost constant values, 15% to 20% in heave and −10% in pitch. Nevertheless, with the DynTD approach, heave factors have been observed within the range of −8% for high pretensions to 8% for low pretensions, as shown in Figure 7 left. Pitch motion with the DynTD approach also shows

increasing factors with a decreasing pretension, as observed in Figure 7 right, though significantly more influenced by lines drag compared with heave.
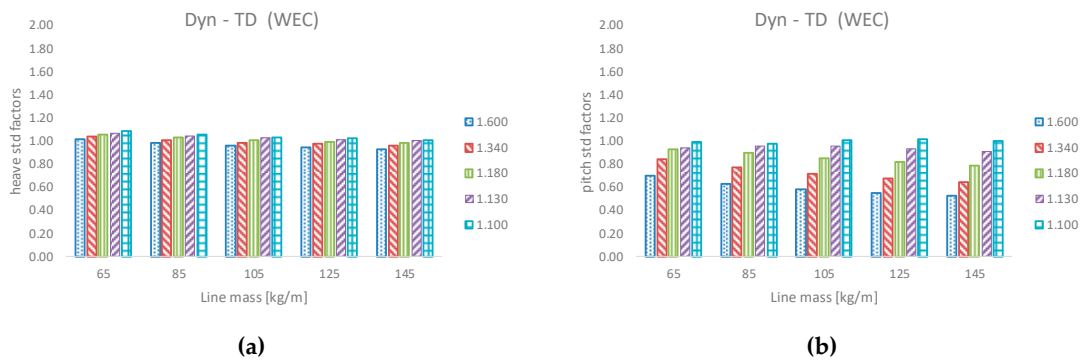

Figure 7. Heaving (**a**) and pitching (**b**) std factors of the DynTD models with respect to the QSFD model.

The increase of the std factor can be explained by looking at the PSDs of each degree of freedom, shown in Figure 8. Surge motion is in general acceptably reproduced by the three models and there is good agreement in the natural frequency among all models, with PSDs showing very good agreement with low non-dimensional pretension. However, mooring systems with large non-dimensional pretensions show damped surge PSDs at the natural frequency with the DynTD models, which can be observed in Figure 8 (left). Heave motion shows factors >1 in all cases as the heaving natural frequency is overdamped, which corresponds with the second peak in Figure 8 (center), with the linearized QSFD model. Even though all time domain models show larger std in heave, DynTD models damp out slightly the heaving motion with respect to the QSTD, resulting in an underestimation of the QSFD and overestimation of the QSTD. Pitching motion std factors are due to the combination of two effects: on the one hand, the QSTD models do not catch entirely the surge-pitch coupling introduced by the mooring system, and on the other hand, large non-dimensional pretension models show damped surge PSDs in the DynTD models in the wave frequency range. Additionally, the QSFD model shows slightly underdamped PSDs in the wave frequency range, with respect to the TD models, which results in the −10% above-mentioned factors of the QSTD models. Therefore, mooring systems with large non-dimensional pretensions introduce significant damping in all degrees of freedom reducing the response, specially in the corresponding natural frequency.
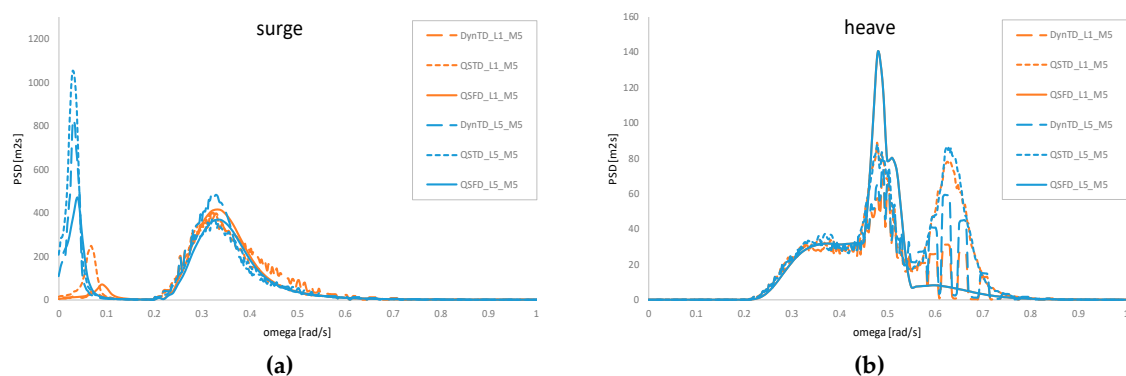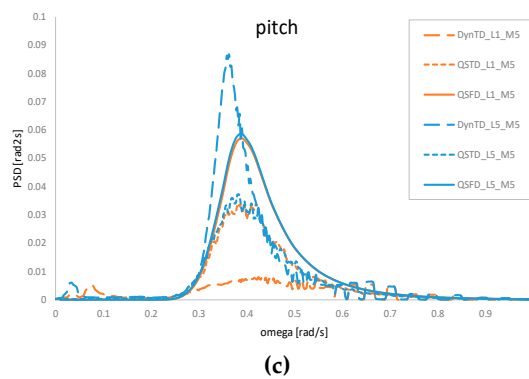

Figure 8. *Cont*.

(c)

Figure 8. Power spectral densities in surge (WF magnified 20 times) (**a**), heave and pitch motions (WF reduced by a factor of 2) (**b**) and (**c**) comparing models' performance with the largest and lowest non-dimensional pretension.

In Figure 9 and Table 4, probability distributions and their corresponding kurtosis (excess kurtosis with respect to the gaussian distribution) and skewness are introduced respectively for surge, heave, and pitch as well as for the most loaded line tension. The kurtosis indicates the higher or lower probability of producing extreme values, respectively, depending if its value is higher or lower than 3, the kurtosis of the Gaussian distribution. In Table 4, the corresponding values of the QSFD models have been omitted since it is a linear model and, therefore, they are Gaussian distributed with kurtosis equal to 3. The skewness indicates the asymmetry of the distribution, Gaussian distributions have zero skewness, and it is also not included.

(a)

(b)

(c)

(d)
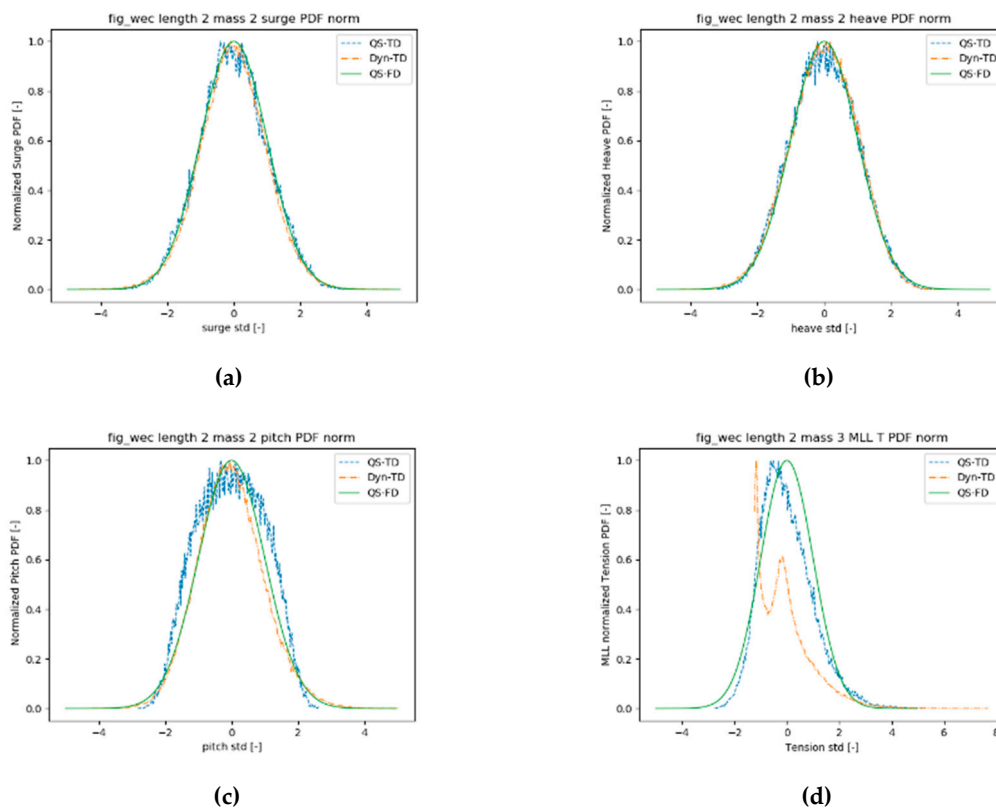
Figure 9. Normalized PDFs with the three models in surge (**a**), heave (**b**), pitch (**c**), and the most loaded line tension (**d**).

All degrees of freedom show negative excess kurtosis and skewness with the QSTD models, with very homogeneous values among the models here assessed, whose mean values are shown in Table 4. Nevertheless, the most loaded line tension shows positive excess kurtosis as well as skewness. It is coherent with the catenary equations as it restricts floater motions through a non-linear increase of line tensions with the offset increase. It therefore leads to lower extreme motion and higher extreme tension values with respect to the linearized QSFD. The most influenced degree of freedom is the pitch motion along with the most loaded line tension, whilst heave and surge do not differ significantly from the equivalent linear PDF, as represented in Figure 9.

Table 4. Mean obtained kurtosis and skewness of the FWEC motions and tension of the most loaded line, obtained with the QSTD approach.

FWEC	Surge	Heave	Pitch	Mll Tension
Kurtosis (QSTD)	2.924	2.671	2.241	3.700
Skewness (QSTD)	−0.188	−0.039	−0.050	0.665

Including lines' drag and inertia, structure motions are modified as already pointed out in the PSD analysis. The heaving motion also shows homogeneous excess kurtosis and skewness among the mooring models with the DynTD approach and its values are shown in Figure 10. Surge, pitch, and most loaded line tensions show variable values depending mostly on the non-dimensional pretension. Surge motion shows higher positive kurtosis with higher pretensions and a kurtosis closer to 3 as the pretension is decreased. The skewness tends towards negative values with lower pretensions and shows a tendency to the values represented with the QSTD approach. It indicates that the fact that the natural frequency is damped out in the PSD of DynTD models; this is due to performing very non-linear motions with high pretensions, making it more difficult to obtain good estimations of extreme surge motions with QSFD models. Pitching motion shows the same tendency as showed by surge and its results have been omitted here for simplicity.
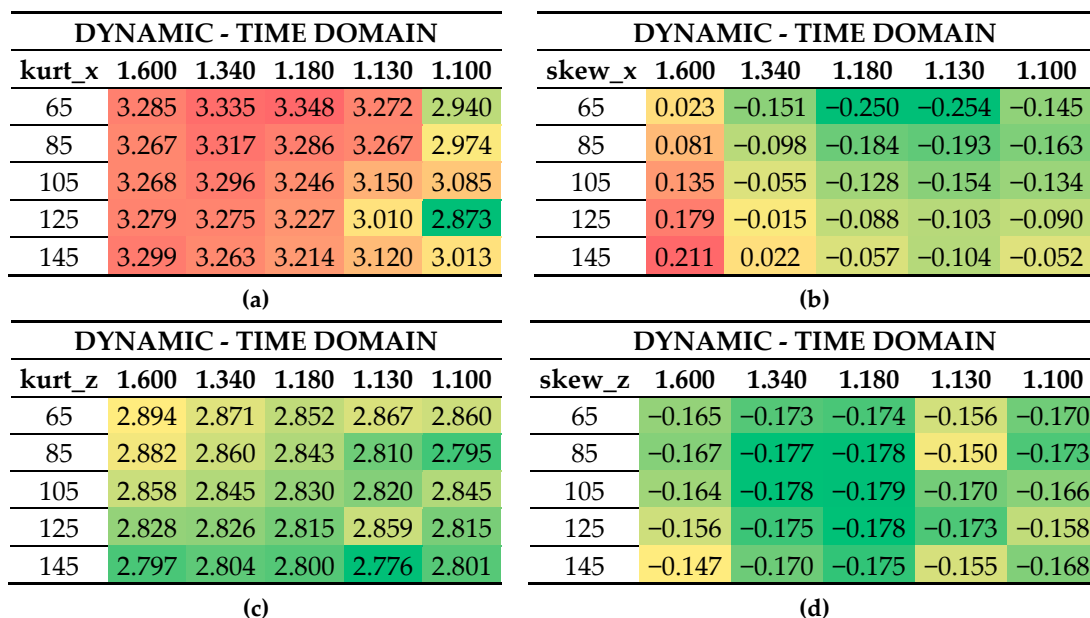
DYNAMIC - TIME DOMAIN					DYNAMIC - TIME DOMAIN				
kurt_x	1.600	1.340	1.180	1.130	1.100	skew_x	1.600	1.340	1.180	1.130	1.100

kurt_x	1.600	1.340	1.180	1.130	1.100
65	3.285	3.335	3.348	3.272	2.940
85	3.267	3.317	3.286	3.267	2.974
105	3.268	3.296	3.246	3.150	3.085
125	3.279	3.275	3.227	3.010	2.873
145	3.299	3.263	3.214	3.120	3.013

(a)

skew_x	1.600	1.340	1.180	1.130	1.100
65	0.023	−0.151	−0.250	−0.254	−0.145
85	0.081	−0.098	−0.184	−0.193	−0.163
105	0.135	−0.055	−0.128	−0.154	−0.134
125	0.179	−0.015	−0.088	−0.103	−0.090
145	0.211	0.022	−0.057	−0.104	−0.052

(b)

kurt_z	1.600	1.340	1.180	1.130	1.100
65	2.894	2.871	2.852	2.867	2.860
85	2.882	2.860	2.843	2.810	2.795
105	2.858	2.845	2.830	2.820	2.845
125	2.828	2.826	2.815	2.859	2.815
145	2.797	2.804	2.800	2.776	2.801

(c)

skew_z	1.600	1.340	1.180	1.130	1.100
65	−0.165	−0.173	−0.174	−0.156	−0.170
85	−0.167	−0.177	−0.178	−0.150	−0.173
105	−0.164	−0.178	−0.179	−0.170	−0.166
125	−0.156	−0.175	−0.178	−0.173	−0.158
145	−0.147	−0.170	−0.175	−0.155	−0.168

(d)

Figure 10. *Cont*.

Figure 10. Kurtosis and skewness of surge motion (**a**,**b**), heave motion (**c**,**d**) and most loaded line tension (**e**,**f**) obtained with the DynTD approach.

4. Predicted Line Tensions

The design line tension has been computed for all cases as defined in Equations (5), (10) and (11). The differences come from the non-linearities included in each model i.e., the non-linear geometric stiffness and line's drag and inertia forces.

The mean line tension shows contributions of 55%–75% on the design line tension and is not significantly sensitive to the mooring settings; the observed differences are driven by line tensions induced by structure dynamics. The QSTD approach shows factors of 1.5 to 2 with a partially increasing tendency with decreasing pretensions in Figure 11. Nevertheless, in contrast to the tendency of structure motions to perform more linear motions with low non-dimensional pretensions, lines' tensions with the DynTD approach show larger discrepancies of the design tension factors as the pretension is increased, of up to 6 with low pretensions, which can be observed in Figure 11. The QSTD approach shows a clear positive skewness and excess kurtosis in accordance with the shape of the catenary curves, as represented in [21]. It is a consequence of both the non-linear stiffness and the coupling with heave, as observed in the PSD of the line tension in Figure 12.
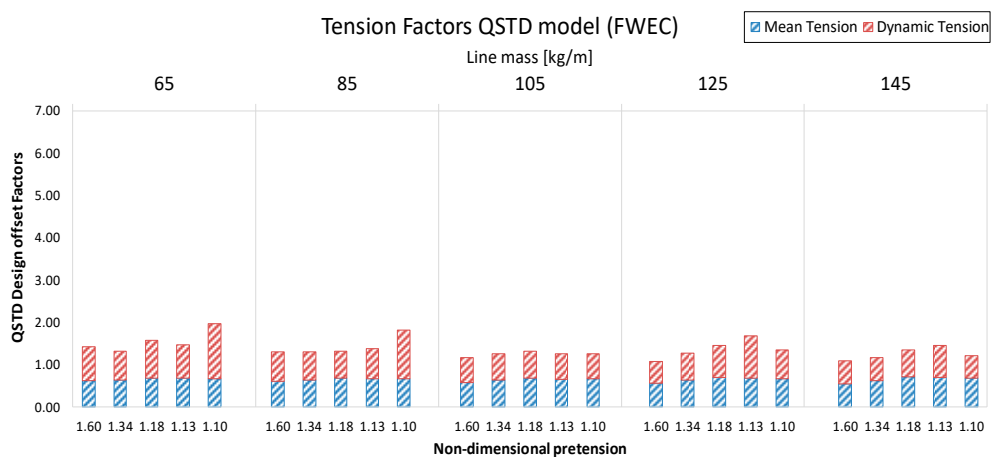
(a)

Figure 11. *Cont*.
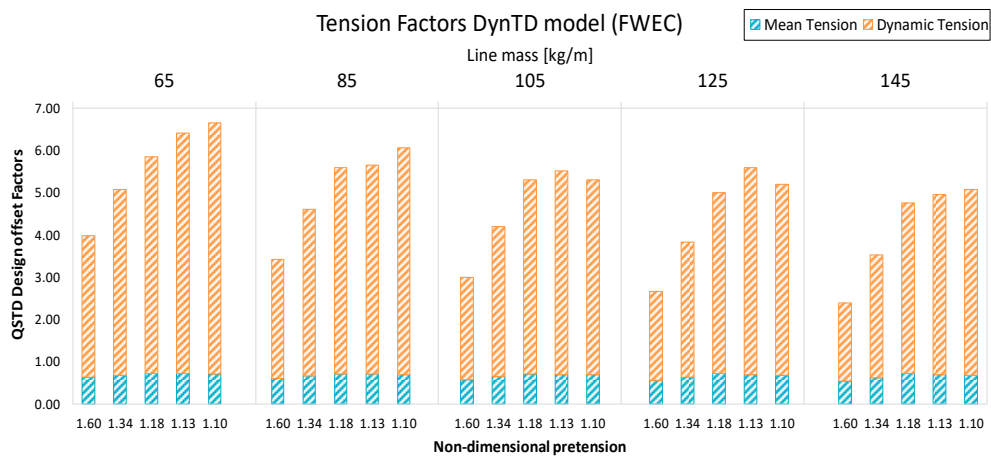
(b)

Figure 11. Most loaded line tension factors for the FWEC with the QSTD (**a**) and DynTD (**b**) models.
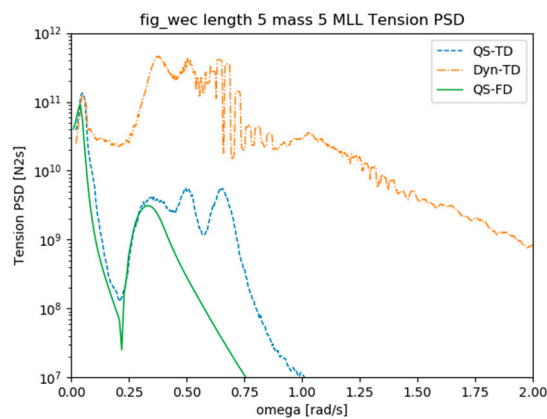

Figure 12. Most loaded line tension PSDs comparisons with the approaches presented.

The most loaded line tensions with the DynTD approach show PDFs with two local maxima as represented in Figure 13. The maximum at higher tensions is due to surge dynamics, which tends to perform more similarly to the QSTD model. However, the peak at lower tensions is due to slack lines during certain instants, which occurs due to the heaving of the buoy and to lines' inertia. It is clearly observed in Figure 14, where a clear correlation of slack line instants with negative heave velocity is observed and not showing a clear correspondence with surge dynamics. In Figure 15, the QSTD approach shows a significant variability in line tension with respect to the quasistatic curve as a consequence of the structure's heaving; however, the DynTD approach shows a very large line tension dispersion due to the lines' inertia, an effect that cannot be reproduced with either the QSFD or the QSTD models, leading to significantly underestimating lines tension. On the other hand, looking at the low frequency range in Figure 12, there is good agreement between the QSTD and DynTD as it appears to be decoupled from the heaving motion.
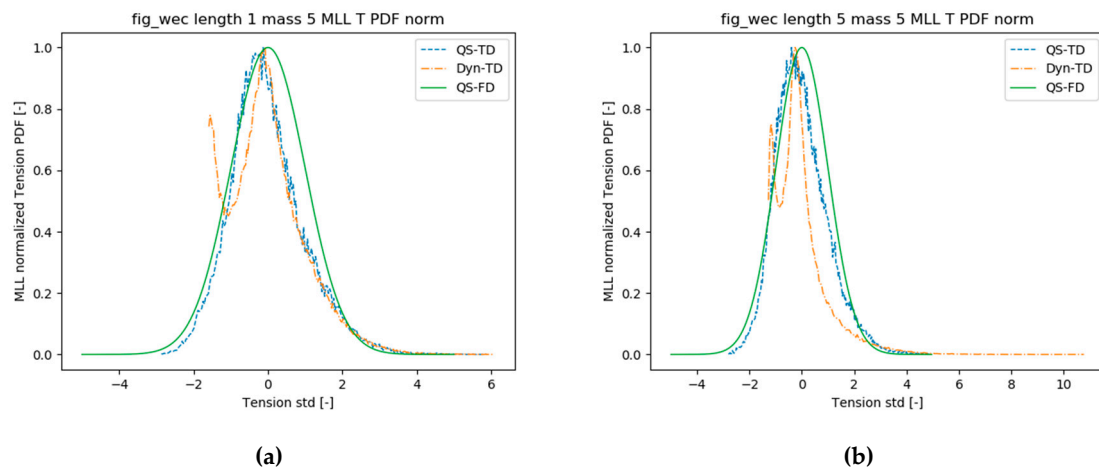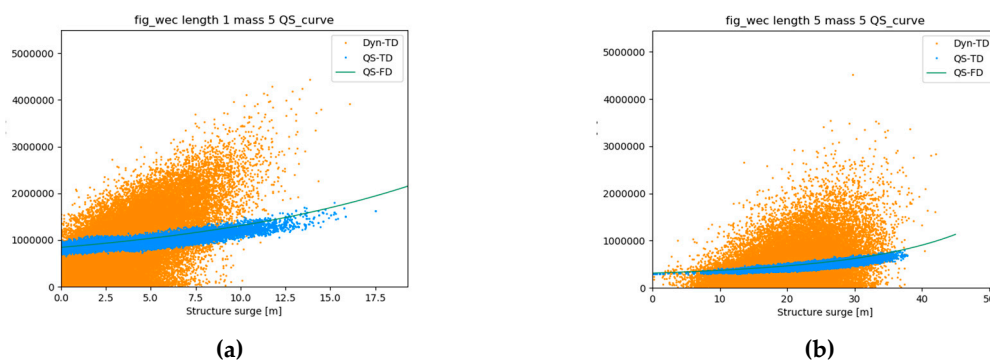
Figure 13. Normalized PDFs of the most loaded line with the three approaches. High pretension (**a**) and low pretension (**b**).
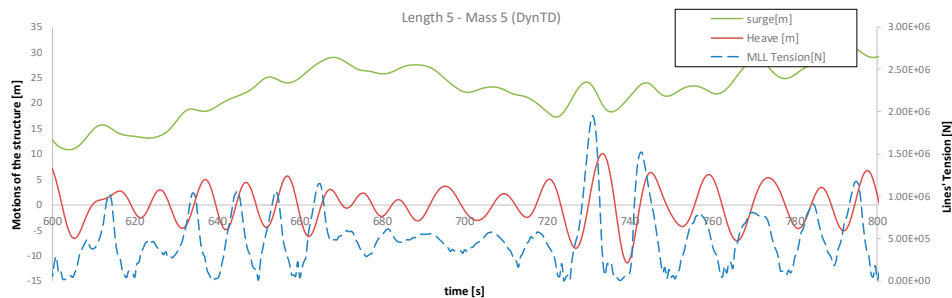
Figure 14. Time series extract of buoy heaving and the corresponding tension of the most loaded line.


Figure 15. Line tension with large pretension (**a**) and with low pretension (**b**) for three models. Green: QSFD, Blue: QSTD and Orange: DynTD.

Consequently, even though the estimation of lines' tension with the QSTD approach shows the influence of the heaving motion with respect to the QSFD, both of them differ significantly with respect to the DynTD with high pretensions mainly due to the lines' induced damping and with low pretensions due to the lines' inertia.

Performance and Cost Comparison Results of Numerical Models

The design results shown in Figure 5 are represented together with the corresponding results obtained with the QSTD and DynTD approaches in Figure 16. Both performance and cost indicators

show the same tendencies with the three approaches. Nevertheless, design line tensions resulting from the DynTD approach are almost one order of magnitude higher and it is to be considered if any of the other two approaches is used at any design stage.


(a)

(b)
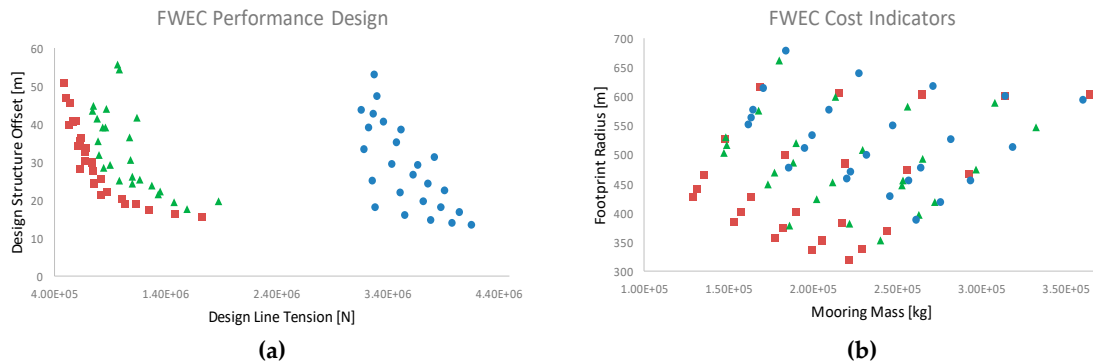
Figure 16. Design (**a**) and cost (**b**) spaces for the FWEC structure with the QSFD (red squares), QSTD (green triangles), and DynTD (blue circles) models.

The mooring total mass and the footprint radius show increasing values as the complexity of the model increases; however, the large impact of lines' drag and inertia observed in the design tension is not translated in a significant increase of the suspended line length and anchor radius. The QSTD approach shows both total mooring mass and anchor radius closer to those of the DynTD than the QSFD, which would make it suitable for mooring design optimizations. However, it does not add significant accuracy improvement in terms of line tensions, and it requires a computational time of the same order of the DynTD.

Given the differences between the QSFD and the DynTD resulting from the linearization and not considering the influence of heave in the QSFD, corrections are proposed in Figure 17 in order to obtain more accurate cost estimations. Since lines pretension have been observed to be more influential on differences between models compared to lines' mass, the corrections proposed here are linear functions of lines' non-dimensional pretension. In addition to the cost indicators, anchor radius, and suspended mass, designers must bear in mind that line tension factors are significant, especially for low pretensions, and corrected line tension should be checked during any design optimization.


(a)

(b)
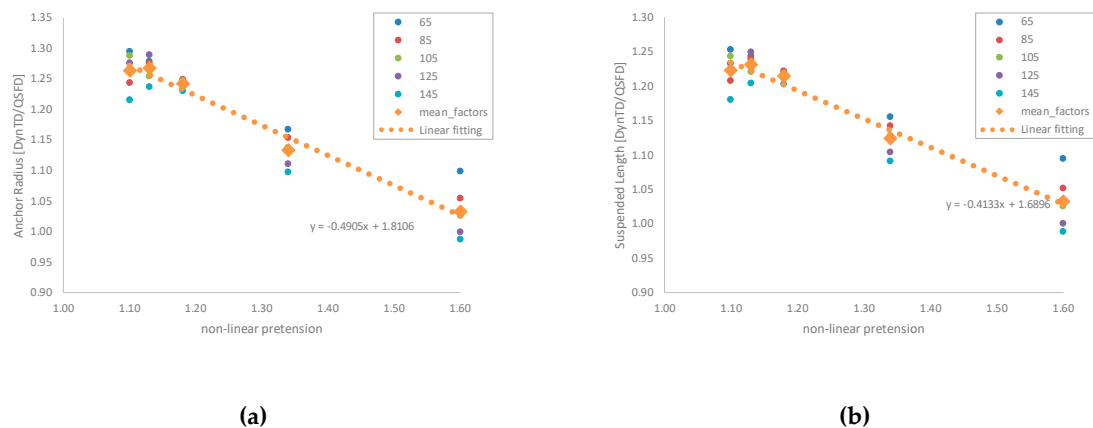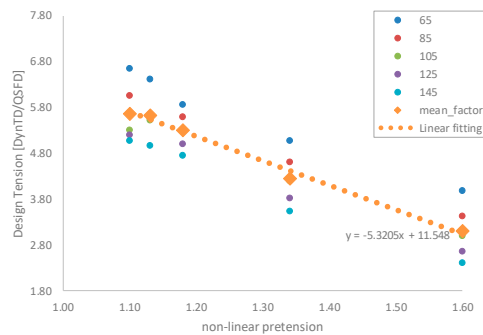
Figure 17. *Cont.*

(c)

Figure 17. Correction factors between the DynTd and the QSFD models for five linear mass values (65, 85, 105, 125, and 145) and a linear fitting of the mean values for Anchor Radius (**a**), Suspended length (**b**) and Design Tension (**c**).

When using these models for mooring design optimization, as described above, QSFD may be used, considering it is corrected following approximation of Figure 17. In order to compare design optimization results of corrected QSFD and DynTD approaches, Figure 18 is introduced. The mooring design optimization has been here considered as the sum of the required area [m^2] and the total mooring mass, computed with the maximum suspended length resulting with each approach and applied to all lines of the mooring system, and the cost has been provided in terms of the total equivalent required mass. The equivalent required mass is the summation of the mooring mass, assuming lines made up of a single chain type, and the equivalent mass of the footprint area given a cost ratio. Assuming a cost ratio of $\frac{\left[\frac{\text{€}}{\text{kg}}\right]}{\left[\frac{\text{€}}{\text{m}^2}\right]} = \frac{3}{1}$, total computed costs represented in Figure 18 with both models result in increasing costs with increasing pretensions independently of the linear mass, and higher optimum linear mass with decreasing pretensions. Figure 18 derives that the QSFD approach seems applicable for early stage optimizations with mid to low linear pretensions, i.e., <1.2. Obtained cost values differ by a 10% and it can acceptably be utilized only for preliminary designs optimizations, setting tendencies of offset, footprint, and total required mass, along with design line tensions, as long as corrections in Figure 17 are accounted for.
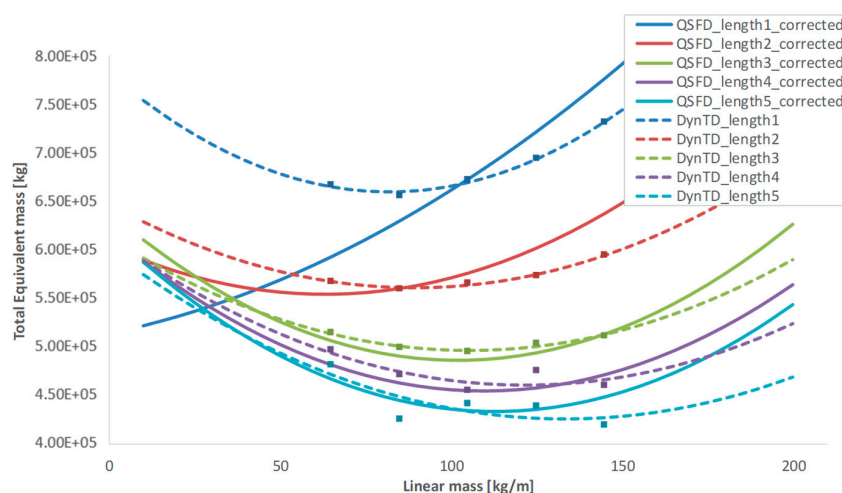
Figure 18. Cost optimization of the mooring system. Total equivalent mass is the sum of 1/3 the lease area and the total mooring mass, assuming a cost ratio of 3 [€/kg]/[€/m^2].

5. Discussion

The QSFD approach shows decreasing design offsets of the structure and increasing design tensions when increasing the pretension, with any linear mass. However, it also implies increasing required footprints and total mass. Even though moderate pretensions have been observed as a mechanism to limit the offset, it has also been showed in Figure 5 that with high pretensions, i.e., >1.2, there is no additional benefit obtained, in terms of offset or footprint, whilst the mooring system is exposed to higher line tensions.

Results of the QSTD and DynTD approaches have been compared with the QSFD baseline results. The design offset, related with the surge motion, shows higher values with the QSTD approach than with the QSFD approach, mainly due to the response in the low frequency range. Its design offsets have been observed in Figure 6 to be driven by the dynamic motions with high pretensions and by the mean offset with low pretensions. Similar tendencies are found with the DynTD approach; however, due to the viscous drag of the lines, the surge natural frequency is significantly damped out with high pretensions and design offsets show increasing factors with decreasing pretensions, showing values, in general, lower than with the QSFD. It means that the QSFD estimates, even though the natural frequency is slightly shifted, are more consistent with the DynTD approach than those of the QSTD, mainly as a consequence of the overdamping introduced by the linearization in the frequency domain, which partially covers lines' viscous drag, accounted for in the DynTD approach. Nevertheless, the QSTD approach reproduces more accurately the low frequency response of the floater and, hence, the corresponding line tension.

Heave motions show larger std values with the QSTD than with the QSFD; the latter uses a linearized viscous drag, which overdamps the heaving natural frequency of the structure. The DynTD approach shows increasing heaving factors with respect to the QSFD approach. Even though heaving PSDs in the natural frequency of the structure are overdamped with the QSFD approach, the peak at a lower frequency (around 0.5 rad/s) shows higher responses, related with resonance of the internal water column. It shows factors of heave std values in Figure 7 increasing from −8% to 8% as the non-dimensional pretension is increased. Pitch motions show the same trend as heaving motions; however, the linearized viscous drag with the QSFD shows an underdamped PSD compared to that of the QSTD and, therefore, QSTD factors are <1. Adding viscous drag forces on lines in the DynTD approach implies, as pointed out for surge and heave, std values close to the QSFD results with decreasing non-dimensional pretension.

In order to assess the degree of linearity of the responses, probability density functions have also been analyzed. As observed in the standard deviations, QSTD approach shows very regular excess kurtosis and skewness among all mooring models, with negative kurtosis and skewness in all degrees of freedom and positive for the most loaded line tension. It is coherent with the catenary equations where small motions imply a non-linear increase of lines tensions, commonly fitted with third order polynomials for practical applications. Heave motion with the DynTD model shows also balanced values among all mooring models, which, together with what is observed in the std values, points at no significant influence of lines' viscous drag and inertia on the heaving motion. On the other hand, both surge and pitch motions are significantly influenced by lines' drag and inertia, resulting in increasingly non-linear PDFs as the non-dimensional pretension is increased. With the DynTD approach all motions show in Figure 10, a tendency to be more linear and closer to the QSFD results in mid to low non-dimensional pretensions, i.e., <1.2.

Looking at the results of the most loaded line tension, factors of the QSTD with respect to the QSFD are not excessively sensitive to the mooring settings, showing std factors of 1.5 to 2 in Figure 11 (left). It has been found to be mainly due to the influence of the heaving motion on lines PSDs as well as the positive excess kurtosis and skewness, introduced by the geometric stiffness. However, the DynTD approach shows, unlike to what is observed in the structure's motions, increasing factors with decreasing non-dimensional pretension, showing values from 3 up to 7 in Figure 11 (right). Even though the higher damping introduced by the viscous drag force on lines with high pretensions is

translated into higher line tensions, mooring models with lower pretensions are increasingly influenced by lines inertia. It is explained looking at the time series showed in Figure 14, where heaving motions moving downwards and upwards with high velocities produce slack lines and the subsequent snap load, respectively. It results in high probabilities of close to zero line tensions as well as of relatively high line tensions. This effect is a consequence of lines inertia, more significative as the pretension is lowered, and can only be reproduced with the DynTD approach.

Mooring cost optimization is most accurate with the DynTD approach, even though the QSTD would provide acceptably good cost indicators, due to the required simulation time of the QSTD and in lieu of any additional accuracy in terms of line tensions, comparison of cost optimisations has been carried out between the QSFD and the DynTD approaches (Figure 18). Both approaches have shown higher total cost and lower optimum linear mass with increasing mooring pretension. Nevertheless, the estimates of the required mass and area with high pretensions are underestimated by the QSFD approach and it has been found to be applicable with mid to low non-dimensional pretensions (i.e., <1.2) to set design tendencies in early stages. The QSFD approach provides a generally underestimated total cost and optimum linear mass that after correction with the functions provided in Figure 17 becomes reasonably usable for early mooring design stages.

6. Conclusions

In the present work, a comparison between three different numerical models of a floating wave energy converter moored by means of a four-line catenary mooring system has been analysed with 25 mooring setting combinations. A linearized frequency domain model (QSFD), a non-linear quasistatic time domain model (QSTD), and a non-linear dynamic model (DynTD) are the three approaches here compared.

A spar type floating wave energy converter (FWEC) has been modelled as a case study. The FWEC has been assumed to be an oscillating water column, working in survivability mode.

The environmental conditions have been assumed to reproduce extreme conditions in the bimep test site. Simulations have been carried out for 25 combinations arising from 5 linear mass and 5 lines non-dimensional pretensions of the mooring system. The selected lines pretension and linear mass have been selected so that realistic buoy offsets are obtained.

It has been found that the influence of viscous drag force on lines is most significant with high non-dimensional pretensions, damping out the natural frequency in all degrees of freedom. It influences most surge and pitch motions; however, its PSDs tend to show more linear motions as the non-dimensional pretension is decreased. The same can be stated for the heaving motion; however, its influence is not significant and the linearized drag force in the QSFD tends to slightly underestimate heaving PSDs. Therefore, buoy motions can be acceptably estimated with the three approaches with low non-dimensional pretensions, while only DynTD is recommended for high pretensions, i.e., >1.2.

Most loaded line tensions show the influence of the heaving motion with the QSTD model and results in slightly higher PSDs than with the QSFD. The QSTD also shows the non-linearity introduced by the geometric stiffness on lines' PDFs increasing the design tension. Nevertheless, heave motions in the DynTD approach induces slack lines and the subsequent snap load cycles and the design line tensions are increased to almost an order of magnitude with respect to the other two approaches. Consequently, as the non-dimensional pretension is decreased, snap loads are more occurrent and line tensions become more non-linear, showing increasingly higher design tensions. Consequently, the most appropriate approach to estimate line tensions is the DynTD approach for line tension estimates in extreme environmental states; however, in cases where only low frequency motions are of interest, the QSTD approach is very consistent with the DynTD for line tension assessment.

Total mooring cost indicators optimizations generally result in higher total costs with higher non-dimensional pretensions and higher optimum linear mass with lower non-dimensional pretensions. Even though the QSTD approach shows more accurate total cost compared with the QSFD, it is not worth being used for early optimizations due to its required computational time, as it does not provide

sufficient accuracy of lines' performance. Found differences in terms of cost and line tension have been found to be mostly functions of non-linear pretensions and linear functions have been proposed so that the QSFD cost and tension results can be acceptably corrected. Therefore, QSFD has proved to show, after applying the corresponding correction factors, acceptable optimization tendencies for non-dimensional pretensions $a_i < 1.2$, while high pretensions require the DynTD approach.

In order to account for operational sea states during preliminary design stages, models that account for lines inertia and drag would be very convenient. Nevertheless, the large number of environmental states and the required simulation lengths and time sometimes may dissuade designers from doing it for a significant number of mooring configurations. Because of its lower computational burden, the frequency domain approach, despite its limitation to capture nonlinear effects, can be corrected with the proposed factors to cover the nonlinear effects and, hence, can be used at early design stages and during concept selection. The authors are currently working on a lumped mass mooring and solid rigid body motions coupled model which, after linearization, can be solved in the frequency domain, accounting for line dynamics to be used under low to moderate environmental states, in which the mooring can be acceptably linearized, keeping the computational cost under the same levels of the QSFD here introduced.

Author Contributions: Conceptualization, I.T. and B.d.M.; methodology, I.T. and B.d.M.; software, I.T.; validation, I.T. and V.N.; formal analysis, I.T.; investigation, I.T., V.N., and V.P.; resources, I.T., V.N., and V.P.; data curation, I.T.; writing—original draft preparation, I.T.; writing—review and editing, I.T., V.N., B.d.M., and V.P.; visualization, I.T., V.N., B.d.M., and V.P.; supervision, V.N. and V.P.; project administration, V.P.; funding acquisition, V.N. and V.P. All authors have read and agreed to the published version of the manuscript.

Conflicts of Interest: The authors declare no conflict of interest.

References

1. OES. News. International LCOE for Ocean Energy Technology. Available online: https://www.ocean-energy-systems.org/news/international-lcoe-for-ocean-energy-technology/ (accessed on 16 March 2020).
2. Offshore Standards. DNVGL-OS-E301: Position Mooring. Edition July 2018. Available online: http://rules.dnvgl.com/docs/pdf/dnvgl/os/2018-07/dnvgl-os-e301.pdf (accessed on 16 March 2020).
3. NI 461 DTO R00 E—Quasi-Dynamic Analysis of Mooring Systems Using Ariane Software. Available online: https://link.springer.com/chapter/10.1007/978-981-15-0291-0_152 (accessed on 16 March 2020).
4. Azcona, J.; Munduate, X.; González, L.; Nygaard, T.A. Experimental validation of a dynamic mooring lines code with tension and motion measurements of a submerged chain. *Ocean Eng.* **2017**, *129*, 415–427. [CrossRef]
5. Hall, M.; Goupee, A. Validation of a lumped-mass mooring line model with DeepCwind semisubmersible model test data. *Ocean Eng.* **2015**, *104*, 590–603. [CrossRef]
6. Touzon, I.; Nava, V.; Gao, Z.; Mendikoa, I.; Petuya, V. Small scale experimental validation of a numerical model of the HarshLab2.0 floating platform coupled with a non-linear lumped mass catenary mooring system. *Ocean Eng.* **2020**, *200*, 107036. [CrossRef]
7. Vu, M.T.; Choi, H.-S.; Kang, J.; Ji, D.-H.; Jeong, S.-K. A study on hovering motion of the underwater vehicle with umbilical cable. *Ocean Eng.* **2017**, *135*, 137–157. [CrossRef]
8. Vu, M.T.; Van, M.; Bui, D.H.P.; Do, Q.T.; Huynh, T.T.; Lee, S.D.; Choi, H.S. Study on Dynamic Behavior of Unmanned Surface Vehicle-Linked Unmanned Underwater Vehicle System for Underwater Exploration. *Sensors* **2020**, *20*, 1329. [CrossRef]
9. Amaechi, C.V.; Wang, F.; Hou, X.; Ye, J. Strength of submarine hoses in Chinese-lantern configuration from hydrodynamic loads on CALM buoy. *Ocean Eng.* **2019**, *171*, 429–442. [CrossRef]
10. Antonio, F.d.O. Wave energy utilization: A review of the technologies. *Renew. Sustain. Energy Rev.* **2010**, *14*, 899–918. [CrossRef]

11. Gomes, R.P.F.; Henriques, J.C.C.; Gato, L.M.C.; Falcão, A.F.O. Hydrodynamic optimization of an axisymmetric floating oscillating water column for wave energy conversion. *Renew. Energy* **2012**, *44*, 328–339. [CrossRef]

12. Doyle, S.; Aggidis, G.A. Development of multi-oscillating water columns as wave energy converters. *Renew. Sustain. Energy Rev.* **2019**, *107*, 75–86. [CrossRef]

13. da Fonseca, F.C.; Gomes, R.P.F.; Henriques, J.C.C.; Gato, L.M.C.; Falcão, A.F.O. Model testing of an oscillating water column spar-buoy wave energy converter isolated and in array: Motions and mooring forces. *Energy* **2016**, *112*, 1207–1218. [CrossRef]

14. Falcão, A.F.O.; Sarmento, A.J.; Gato, L.M.C.; Brito-Melo, A. The Pico OWC wave power plant: Its lifetime from conception to closure 1986–2018. *Appl. Ocean Res.* **2020**, *98*, 102104. [CrossRef]

15. Marine Energies—EVE. Available online: https://eve.eus/Actuaciones/Marina?lang=en-gb (accessed on 6 June 2020).

16. MARMOK-A-5 Wave Energy Converter. Tethys. Available online: https://tethys.pnnl.gov/project-sites/marmok-5-wave-energy-converter (accessed on 6 April 2020).

17. Nielsen, K.; Wendt, F.; Yu, Y.H.; Ruehl, K.; Touzon, I.; Nam, B.W.; Kim, J.S.; Kim, K.-H.; Crowley, S.; Sheng, W. OES Task 10 WEC heaving sphere performance modelling verification. Presented at the 3rd International Conference on Renewable Energies Offshore (RENEW 2018), Lisbon, Portugal, 8–10 October 2018.

18. Wendt, F.; Nielsen, K.; Yu, Y.H.; Bingham, H.; Eskilsson, C.; Kramer, M.; Babarit, A.; Bunnik, T.; Costello, R.; Crowley, S. Ocean Energy Systems Wave Energy Modelling Task: Modelling, Verification and Validation of Wave Energy Converters. *J. Mar. Sci. Eng.* **2019**, *7*, 379. [CrossRef]

19. Penalba, M.; Mérigaud, A.; Gilloteaux, J.-C.; Ringwood, J.V. Influence of nonlinear Froude–Krylov forces on the performance of two wave energy points absorbers. *J. Ocean Eng. Mar. Energy* **2017**, *3*, 209–220. [CrossRef]

20. Pinkster, J.A. Mean and low frequency wave drifting forces on floating structures. *Ocean Eng.* **1979**, *6*, 593–615. [CrossRef]

21. Touzon, I.; de Miguel, B.; Nava, V.; Petuya, V.; Mendikoa, I.; Boscolo, F. Mooring System Design Approach: A Case Study for MARMOK-A Floating OWC Wave Energy Converter. Presented at the ASME 37th International Conference on Ocean, Offshore and Arctic Engineering, Madrid, Spain, 17–22 June 2018. [CrossRef]

22. Fitzgerald, J.; Bergdahl, L. Including moorings in the assessment of a generic offshore wave energy converter: A frequency domain approach. *Mar. Struct.* **2008**, *21*, 23–46. [CrossRef]

23. Larsen, K.; Sandvik, P.C. Efficient Methods for the Calculation of Dynamic Mooring Line Tension. Presented at the First ISOPE European Offshore Mechanics Symposium, Seoul, Korea, 24–28 June 1990.

24. Low, Y.M.; Langley, R.S. Time and frequency domain coupled analysis of deepwater floating production systems. *Appl. Ocean Res.* **2006**, *28*, 371–385. [CrossRef]

25. Cummins, W.E. The Impulse Response Function and Ship Motions. Presented at the Symposium of Ship Theory, Hamburg, Germany, 25–27 January 1962; Institut für Schiffbau der Universität Hamburg: Hamburg, Germany, 1962.

26. van den Boom, H.J.J. Dynamic Behaviour of Mooring Lines. In Proceedings of the Behaviour of Offshore Structures, Delft, The Netherlands, 1–5 July 1985; Elsevier Science Publishers B.V.: Amsterdam, The Netherlands, 1985.

27. OrcaFlex. Dynamic Analysis Software for Offshore Marine Systems. Available online: https://www.orcina.com/orcaflex/ (accessed on 15 December 2019).

28. Naess, A.; Moan, T. *Stochastic Dynamics of Marine Structures*; Cambridge University Press: Cambridge, UK, 2012.

29. Metocean Analysis of BiMEP for Offshore Design TRLplus. IH-Cantabria, bimep, 2017. Available online: https://trlplus.com/wp-content/uploads/2017/03/Metocean_Analysis_of_BiMEP_for_Offshore_Design_TRLplus_March_2017.pdf (accessed on 19 March 2020).

30. MATLAB. El Lenguaje del Cálculo Técnico. MATLAB & Simulink. Available online: https://es.mathworks.com/products/matlab.html (accessed on 5 July 2020).

31. DNV-RP-C205. *Environmental Conditions and Environmental Loads*; Det Norske Veritas: Oslo, Norway, 2010.